# 3D Visualization of Vessels and Tumors for Guidance in TACE

Lukas Huber, Musfira Naqvi, Chantal Pellegrini

22.07.2021

## 1 Introduction (Lukas Huber)

Liver cancer is the fifth most diagnosed, but second most cancer-related death in the world for men. For women, it is the seventh most diagnosed cancer and sixth leading cause of cancer-related death, indicating a 2-3 times higher prevalence for men than women [7]. While the were 748.000 new cases in 2008 [16], the number increased to 841.000 in 2018 [7]. During 1975 and 2014 the prevelance more than tripled across the world [18]. Liver cancer is especially prevalent in transitioning and lower HDI countries, where it actually is the most common type of cancer. Highly affected regions include Eastern and South-Eastern Asia, Micronesia, West and Central Africa and Egypt [7]. Common causes for liver cancer are a hepatitis B/C (HBV/HCV) infection, alcoholism, aflatoxin contaminated food, obesity, smoking, type 2 diabetes and parasitic liver flukes [4]. The most common cause drastically differs from country to country. While a HBV infection and aflatoxin intake trough food are the main causes in Latin America, alcoholism and a HCV infection is the leading cause in the United States, Europe and Japan [17]. While the rollout of a HBV vaccine will prevent many liver cancer cases in the future, the exists no effective vaccine against HCV to this date [9]. Increasing obesity will increase the prevalence further, especially in higher HDI countries [3]. In total, around 73% of all liver cancer cases are caused by HBV, HCV and parasitic liver flukes [27].

Hepatocellular carcinoma (HCC) accounts for 75% to 85% of all liver cancers and is a malignant tumor. Symptoms are usually developed at an advanced stage which makes it hard to diagnose. For patients with cirrhosis, it even is the leading cause of death. Common symptoms are abdomoinal pain and swelling, weight loss, general weakness, loss of appetite, fewer and jaundice. It remains one of the most fatal cancers with a 5 year survival rate of less than 20%. [17]

Only about a third of the patients can be treated with currative methods like transplantation or resection, mainly due to the typically late diagnosis of the HCC [17]. Transarterial chemoembolization (TACE) is a minimally invasive operation to treat intermediate stage, unresectable HCC and is often the therapy of choice for palliative treatment [8]. It may be applied on tumors that are either not treatable via ablation or as bridging therapy to keep tumor size small until a transplant [29]. Figure 2 shows the available treatment options for a HCC according to the *Barcelona Clinic Liver Cancer* (BCLC) staging [24]. A hepatocellular carcinoma grows many blood vessels which are supplied by the proper hepatic artery. The healthy liver tissue, on the other side, is supplied by the portal vein [42],


(a) Before TACE (b) After TACE

Figure 1: HCC carcinoma before and after the TACE procedure. Taken from [29].

which is an important reason why TACE works in practice. The TACE procedure combines both local chemotherapy and embolization to reduce tumor growth and eventually shrink it [22]. It was shown that the intratumoral concentration of the agent is around ten times higher than in the surrounding tissue when applied via the hepatic artery compared to the portal vein [12].

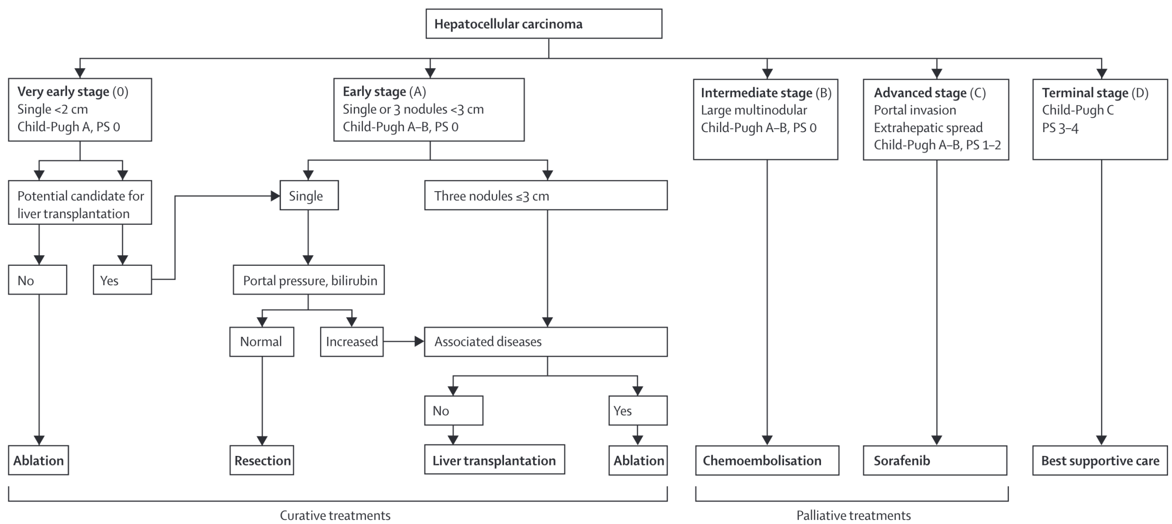


Figure 2: Treatment strategy for HCC according to the BCLC system [24]

During the procedure, the surgeon injects a catheter from the groin into the femoral artery using the Seldinger technique, guiding it into the hepatic artery. For navigation a combination of pre-operative CT-scans and fluroscopy is used. A contrast agent is used to create an angiogram, needed to detect branches of the artery feeding the tumor. During the procedure, the contrast agent needs to be reapplied multiple times. A micro catheter is then used to navigate to the optimal position close to the tumor. The actual treatment then consists of an injection of a chemoterapeutic agent like doxorubicin, cisplatin or mitomycin, which only acts locally on the tumor. In comparison with a systematic chemoterapeutic treatment this leads to less side effects and the possibility to apply a higher dose. Further, the tumor feeding vessels are blocked using a embolization agent like Lipiodol, Gelfoam or microspheres. The intra-aterial injection leads to strong cytotoxic effect and ischemic necrosis. Once neovascularization (i.e. regrowth of new blood vessels by tumor as reaction on ischemia) occurs, TACE can be applied again. [38, 29]

While the total costs vary between different countries, several studies report an average cost between 17,000$ [34] and 13,418€ [11], depending on the country and hospital. Since TACE is often applied multiple times, the overall cost can vary from case to case. In a randomised controlled trial, TACE showed improvements in the 1 and 2 year survival rate with 82% and 63% compared to 75% and 50% for embolization only. The control group receiving conservative treatment showed survival rates of 63% and 27% [22].

During the operation, the surgeon has to navigate the catheter to the optimal spot in the blood vessel to perform the chemoembolization. Since the exact anatomy of the blood vessels can differ drastically between patients, this is not a straightforward task. In a normal operation setting, the surgeon combines information from the current catheter position in the angiogram with a preoperative contrast CT. Even with this combined information, the navigation task can be very time consuming. To ease this process, we propose a 3D visualization of the blood vessel structure such that the surgeon can directly observe the structure and branching of the vessels. Our solution comes with no extra cost since it extracts the vessel structure from a preoeprative contrast CT scan, which is usually already performed for operation planning. Further, our solution is simply an additional visualization during surgery and therefore comes with very little risk for the surgery.

## 2 Related Work (Lukas Huber)

The system that matches our solution the most is called *EmboGuide* and marketed by Phillips [2, 1]. It is a standalone solution and relies on the *XperCT Dual* multiphase cone beam CT and a interventional X-Ray like the *AlluraClarity* system, both manufactured by Philips. It was shown by a study that the lesion detection by the *XperCT Dual* system is on par with that of Magnetic Resonance Imaging (MRI), the so-called gold standard [28]. It offers a live 3D navigation for the catheter to reach the optimal point in the vessel structure for the chemoembolization. Compared to standard 2D imaging alone, like an angiogram, it allows the surgeon to navigate the catheter easier. It is further able to detect and segment the tumor and its feeding vessels. Compared to the conventional digital subtraction angiography (DSA), Philips claims to detects 50% more feeding vessels [35]. In addition to pure visualization, the vascular tree is overlaid by the pre-planned route. [2, 1]

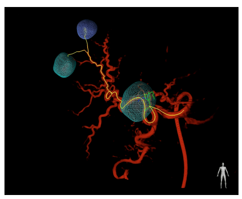

(a) Feeding vessel detection by Emboguide [1]

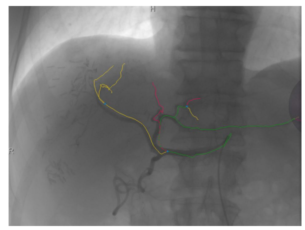

(b) Overlay of the vascular structure by the live fluroscopy image

Figure 3: Imaging methods offered by the EmboGuide [2] and Syngo [39] system.

The Syngo Embolization Guidance system offered by Siemens has a very similar feature set to the Emboguide [39]. It relies on a contrast-enhanced Cone-beam CT (e.g. the Syngo DynaCT). The Syngo Embolization Guidance system allows to detect the catheter currently present in the hepatic artery. Starting from that position, a vessel tree can be computed that only consists of feeding vessels supplying a predefined lesion. The distances to the lesion is encoded by different coloring of the individual blood vessels using a set of predefined colors. The automatically created vascular tree can further be refined in a way that single vessels can be removed by selecting a vessels branch. The user can also mark a lesion by drawing a line trough it defining the diameter, requiring only a single input. This creates a circular lesion visualization including a configurable safety margin. The system is designed in such a way, that the surgeon does not need to leave the interventional room for interaction with the system. Lastly, the manufacturer highlights the reduction of the overall radiation dose during the operation. [32]

The *Flightplan for liver* software distributed by GE healtcare offers a 3D visualization of the vascular tree, which automatically detects up to 93% of the tumor feeding vessels in the liver compared to only 64% when using 2D imaging alone [15]. It can be used for both the preoeprative planning of the TACE oepration and during surgery to guide the catheter [15, 19, 20, 40].

The Department of Health & Human Services in the United States considers the Philips *EmboGuide* and Siemens *Syngo* system equivalent in design features, fundamental scientific technology, indications for use, safety and effectiveness. It further sees the vascular tree visualization of the *EmboGuide* as comparable to the *Flightplan for liver* [31].

In addition to the mentioned products already marketed by Siemens and Philips, there exists interesting work in academia related and useful for our approach. With their *Graph Cut Liver Segmentation* approach, Esneault et al. [14] offer a way to create a graph cut based segmentation of the liver from a CT scan. This includes the liver tissue, the vascular tree and the tumor. They model the segmentation task by a directional flow graph and apply the Max-Flow/Min-Cut algorithm to extract two subsets: The voxels corresponding to the *background* and the ones *defining the objects of interest*. Since the approach is semi-automatic, the user first needs to manually select a set of voxels that correspond to the object of interest. Further, a set of voxels corresponding to the background need to be defined. The algorithm can then extract the segmentation corresponding to the selected object. In order to obtain segmentations for the vascular structure, the tumor and the liver, the algorithm can be iteratively queried with different sets of seed voxels picked by the user. On the downside, such an approach might lead to discontinuities, especially at branchings. [14]

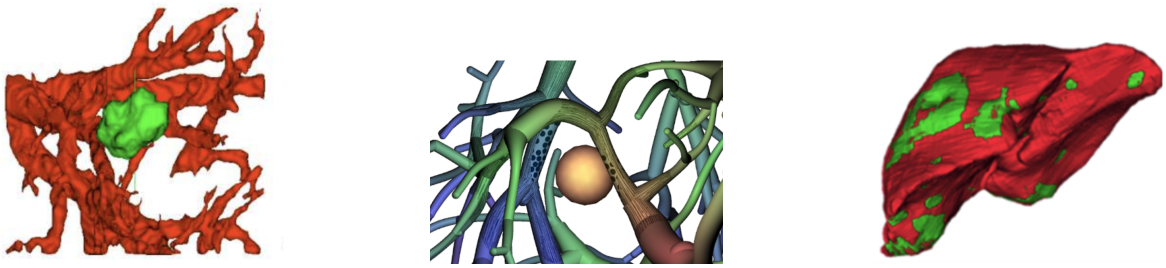

Figure 4: Left: Vessel and tumor segmentation by [14]. Middle: Improving vessel visualization using color, texture and hatching [30]. Right: 3D liver segmentation by [43].

Zhang et al. [43] propose a solution for liver and liver tumor segmentation using an improved V-net model [25], which is a 3D variant of the popular U-Net architecture [33]. Our proposed approach creates a 3D visualization of the vascular structures of the liver. One needs to keep in mind that the usefulness of the visualization heavily depends on how the vessels are presented on the screen. One needs to especially consider the problem of perceiving spatial depth and vascular properties such as branching level. Ritter et al. [30] propose a set of techniques to improve over the mentioned problem of the perception of a regular vascular tree structure. In order to optimize the visualization of shape, the authors propose the use of hatching, which is done along the curvature directions. Texture is used as an additional attribute to encode information about distances between vascular structures, shape and spatial orientation and also the distance to other organs. Combined with color, these attributes can also be used to encode information about the type of the vessel (i.e. artery or vein), diameter of the vessel and branching level.

# 3 Surgical Workflow (Musfira Naqvi)

In the following the surgical workflow of TACE is displayed within figure 5 and 6.
The workflow of both the attending nurse as well as the surgeon is shown simultaneously.

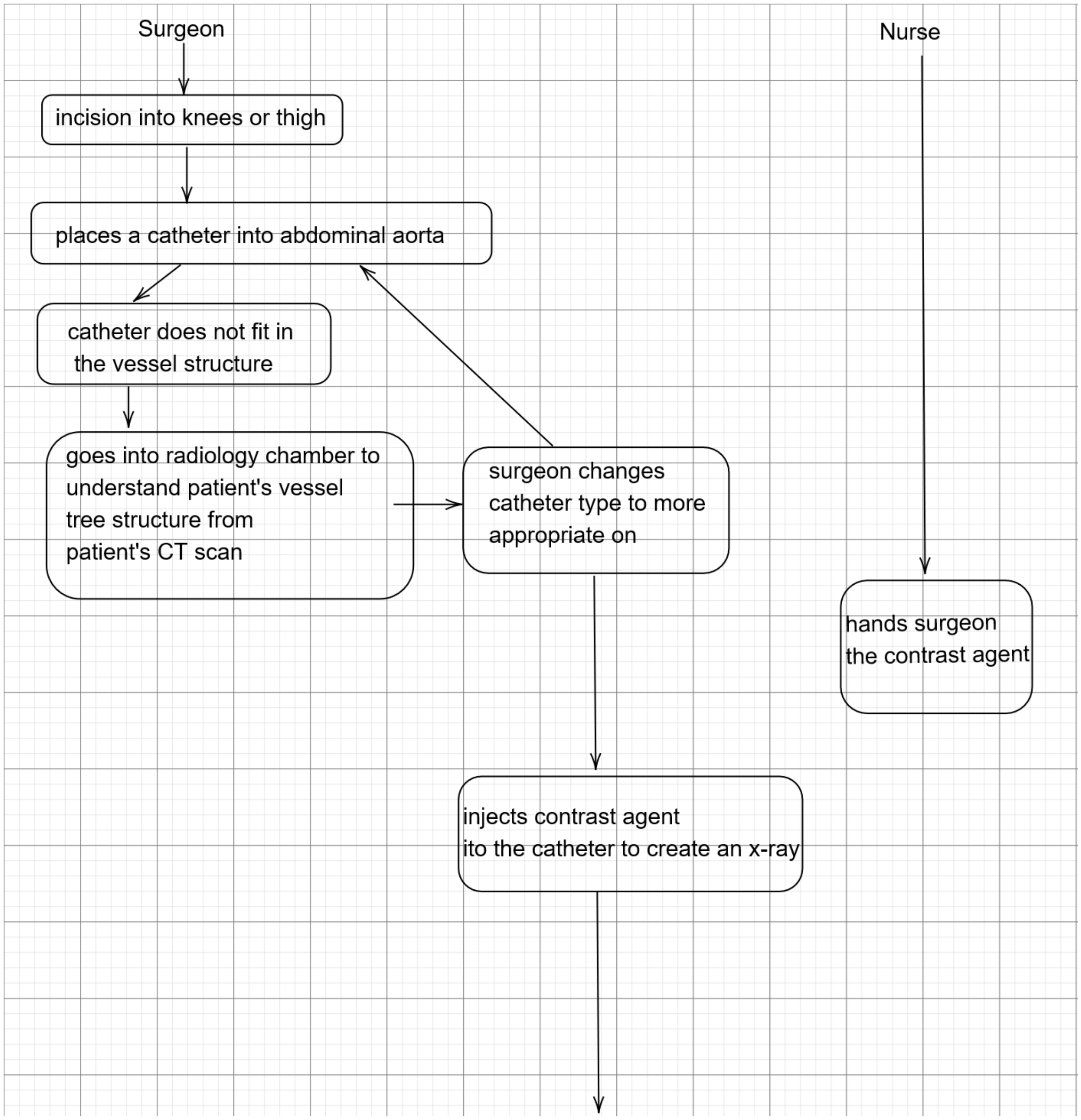


Figure 5: Workflow Part 1

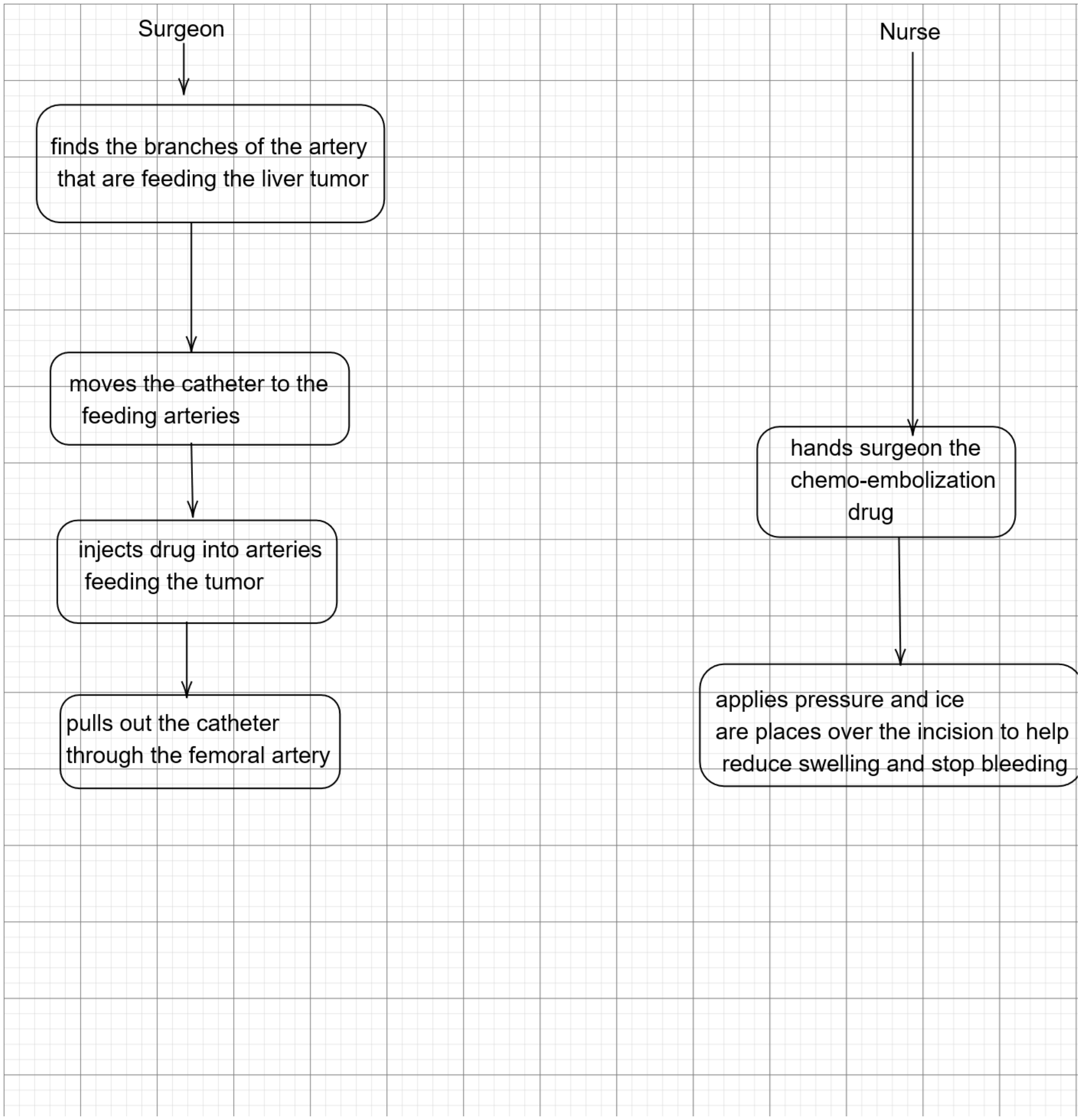


Figure 6: Workflow Part 2

# 4 Problem Statement (Musfira Naqvi)

It is important to note, that for TACE, selective catheters are used. Selective catheters are designed for rotational stiffness, which makes it easier to manipulate the catheter's trailing end position. There are several types of selective catheters:

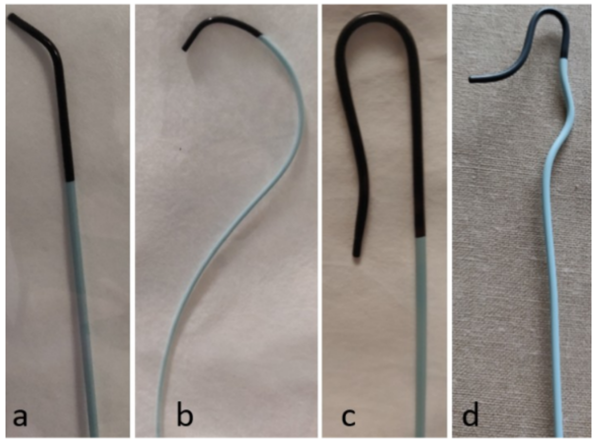


Figure 7: a) Bernstein catheter b) Cobra 1 catheter c) SOS catheter d) Mickelson catheter [6]

In figure 4, a picture of [6] shows different catheter types of which the interventionist has to choose from. The choice of selective catheters depends on the size and shape of the targeted vessel.

While it is not a problem for the surgeon to position the catheter within the veins, it is a challenge to initially decide for the correct catheter type to be used for the procedure.
For instance, during our observation, the surgeon started the procedure with the cobra catheter. However the cobra catheter could not enter the targeted vein as the angle of the ramification was too sharp. Therefore a different catheter was needed where the angle between catheter and catheter tip is small.
Because of that, it became impossible for the surgeon to continue the insertion of the catheter and therefore needs to remove.
Simultaneously it is important for the surgeon to have a correct understanding of the vessel structure and the tumor location. This is needed in order to find an optimal position for the chemo-embolization process. Goal of this procedure is to save as much healthy liver tissue as possible as well as blocking the blood supply to the tumor.
In order to then decide for an appropriate catheter and to check for the catheter's optimal positioning, the surgeon had to leave the OR room multiple times to enter the radiology cabinet. There, he discussed the patient's CT scan with the radiologist to get a mental image of the patient's vessel tree structure and also to ensure the catheter's correct positioning.
It became apparent, that not knowing the patient's vessel tree during the procedure complicated the procedure and at the same time elongates surgery time. Furthermore, it causes discomfort on the surgeon's side, as he will wear a heavy lead protective. At the same time, the elongated procedure also causes distress to the patient - who is in an awake state - as they want everything to go as smoothly as possible.
To quickly summarize: Because of the fact, that the patient's anatomy can differ, different catheter have to be used for TACE. In order to understand which catheter is supposed to be used by the surgeon, the surgeon needs to understand the vessel tree structure of the patient. However to combat the liver tumor with the best results it is important to find the catheter positioning for chemo-embolization. It is because of this, that this paper proposes the visualization of the vessel tree during TACE.

# 5 Proposed Technical Solution (Chantal Pellegrini)

To improve the surgical workflow of TACE, we propose to build an easily readable 3D visualization of the vessel structure and the tumors of the patient. This visualization can be used for surgery planing as well as for orientation and decision making during the procedure. An intraoperative display of the

visualization enables a fast information lookup and its orientation is meant to be controllable by the surgeon.
To create this visualization we only rely on the preoperative contrast CT scan, which is usually performed before a TACE procedure. Given this CT scan, the creation consists of several steps:

**Vessel Segmentation** The vessels supplying the liver are segmented in the 3D CT volume.

**Vessel Analysis** The segmented vessel tree is split in the hepatic artery and portal vein using a graph-based analysis.

**Liver and Tumor Segmentation** The liver and the tumors inside the liver are segmented from the CT scan.

**Visualization** A 3D visualisation of the tumor and the vessel tree is embedded in a direct volume rendering of the preoperative CT scan.

Furthermore, we want to enable the surgeon to adapt the visualisation, firstly to verify it and secondly to decide which information he wants to have displayed for the current patient.

## 5.1 Imaging Methods and OR Setup

We designed our method in a way that ensures minimal changes in the current surgical workflow and operating room setup. The entire visualization is based on the usual preoperative contrast CT-scan. The best contrast for the hepatic artery and HCCs is provided during the arterial phase, so a CT captured in this phase should be used as input for the segmentation methods. The visualisation is meant to be displayed on an extra screen in the operating room next to the intra-operative angiography. For convenience the screens should be positioned behind the operating table in front of the surgeon, but this is not vital for our approach. The surgeon has to be able to control the 3D rotation of the visualisation. In the operation we visited, the surgeon already had buttons with which he could control the images on the screens. Here another controller could be added. As our visualisation is static, no additional imaging or computation has to be performed intraoperatively.

## 5.2 Vessel Segmentation and Analysis

One possible approach to segment the vessel tree was proposed by Yang et al. [41]. They applied an adapted version of V-Net [26], which is a fully convolutional neural network developed for 3D image segmentation. After segmentation small area noise is removed in a post-processing step. For training and testing the 3D Image Reconstruction dataset 3Dircadb is used [23]. If there is too little data available, it could work better to use a 2D segmentation method instead. One possible method here is the VesselNet [21], which predicts a vessel probability for each voxel given patches on the sagittal, coronal and transverse plane centered on the current voxel. The features for all three patches are extracted using three separate convolutional networks and then combined with a fully connected layer. On the segmented voxels, a graph-based analysis as described in [36], can be performed. The segmentation is skeletonized and transformed into a graph, in which the vertices represent ramifications and the edges represent connecting vessels. Given this data structure the geometry and ramification structure can be analyzed, allowing to automatically distinguish between the portal tree and the hepatic artery. This step is not necessary for VesselNet as this method only segments the hepatic artery. Nevertheless the graph creation is needed for the visualization in the end.

## 5.3 Liver and Tumor Segmentation

For segmenting the liver and the tumors there are again methods working on the 3D volume as well as on 2D slices. Zhang et al. [43] proposed a liver and tumor segmentation method, which directly works on 3D CT volumes. The proposed method builds upon V-Net, adapting it by altering the loss

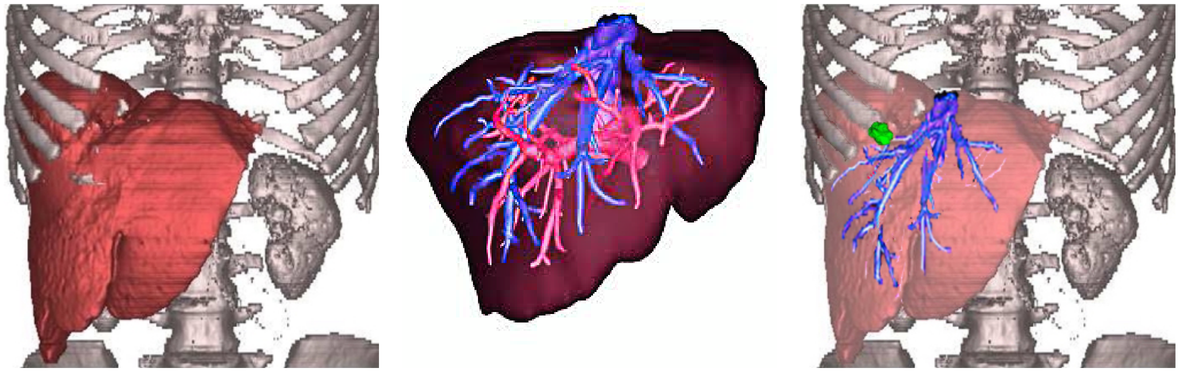

Figure 8: left: direct volume rendering of abdominal CT with highlighted liver [13], middle: vessel visualization of portal and hepatic tree described by Selle et al. [36], right: conceptual visualization of vessels and tumor (green) in the semi-transparent liver segmentation embedded in the CT rendering.

function used for training. It can be used for both, liver and tumor segmentation, without the need for adaptation. The algorithm was tested on two datasets, LiTS17 [10] and 3Dircadb [23], showing good performance for both liver and tumor segmentation.
As 2D alternative for instance the method proposed by Ayalew et al. [5] can be used. They propose a modified version of U-Net which can be trained for both liver and tumor segmentation on slices of CT scans.

### 5.4 Visualization

The segmentation of the liver, the vessel tree and the tumor regions are ported into a 3D visualization. This visualization can be placed inside a rendering of the CT volume, so the surgeon can better understand where in the abdomen the vessels and the tumors are located. Also the visualization of the liver serves as aid for understanding the structural context. For rendering the CT data we propose to apply direct volume rendering, so the full data can be observed at once. There already exists software providing the capabilities to perform direct volume rendering and most radiology departments have the respective software [37]. To visualize the liver and the tumors, the segmented voxels need to be highlighted with different colors. The segmentation of the liver needs to be displayed transparent, so the full vessel structure and the tumors can be seen. A possible way to visualize the vessel tree is described in [36]. Here several truncated cones are expanded along paths from the tree root until the leaves of the graph created during vessel analysis. Figure 8 shows examples for the CT volume rendering and the vessel and tumor visualization.

### 5.5 Quality Control and Configuration through surgeon

Our solution is meant to be used as an extension to the current imaging provided. The surgeon knows the CT-scan and by comparing it with the visualization he can detect critical errors. This step avoids confusion during the surgery in case the visualization differs too much from the expected vessel structure.
The tumor segmentation may detect more than one tumor region in the liver. Here we want to make it possible to hide some of these tumors. During a TACE the surgeon might not want to target all tumors in the liver, so it is sufficient and clearer to only show the targeted tumor or tumors. To separate the different tumors inside the segmentation, a simple connectivity-based clustering with a appropriate distance threshold can be used, as it is sufficient to separate tumor regions which are comparatively far apart in space.

## 6 Risks and Drawbacks (Chantal Pellegrini)

As our proposed visualization is performed preoperatively, no unexpected failures should occur during the surgery, which is immensely limiting the potential harm which can be caused by our application. Like with every technical solution the screen and screen controllers can theoretically fail. However, as we rely on the currently available equipment of the operation room this is highly unlikely and would affect not only our application but the whole imaging system, which would in any case lead to an interruption of the surgery.

The main risk for errors lies in the preoperative creation of our visualization using automated segmentation techniques. Both vessel and tumor segmentation from CT scans are non-trivial tasks and the methods we propose to use will not result in perfect segmentations. A wrong segmentation leads to a wrong presentation of the vessel structures and tumor position and thus the surgeon will have an incorrect perception of these structures. This inhibits the surgeon to correctly plan and perform the surgery. For this reason we do not propose that the surgeon solely relies on our visualization outcome, but rather uses it to improve his understanding of the CT scan by facilitating a good 3D understanding of the structures. As surgeons performing this procedure are trained in understanding the plain CT scan they will notice if the visualisation has a significant error during a quality control of the visualization. In this case they can fall-back on planning and performing the surgery only using the CT scan.
For smaller errors the implications are less grave. As our visualization primarily should be used to gain a better understanding of the vessel structures and the tumor regions, small segmentation errors of a few voxels can be ignored. These will only lead to a slight displacement of the tumor and vessel boundaries without changing the overall structure. Other minor errors include false positives during the tumor segmentation. In case they result in wrong tumor regions this can be corrected by the surgeon during the configuration phase.

One drawback of the proposed method is that it relies on a manual quality control, leading to additional work for the surgeon. Nevertheless this still yields less effort than manually segmenting the CT scan or providing an initial segmentation for a semi-automated segmentation method like proposed by Esneault et al. [13]

There are several systems like the EmboGuide and the Syngo Embolization Guidance system, which provide the surgeon with a live guidance, that can be used intraoperatively for catheter road-mapping. This highly differs from our proposal as we want to show the surgeon a static visualization, which is not updated during the surgery. Through using a static visualization we provide less information for the surgeon, for instance no information about the live catheter position. During our surgery visit we perceived the catheter navigation during TACE as a rather straightforward step, as the catheter position is determined by the vessel walls. Also the surgeon did not seem to have difficulties understanding the catheter position from the 2D angiographic image. Nevertheless without visualizing the catheter, the surgeon has to still use the angiographic imaging, so he has to consider several images at once, which can be tiring. Also he has to mentally map the information on the angiogram to the information provided by us. For a less experienced surgeon this could be non-trivial. Nevertheless, in the operation we observed, the surgeon was using the preoperative CT scan as reference, so he had to perform this mapping as well. It did not seem as if this mapping was leading to problems for him.
Given that we rely on automated segmentation, whereas the EmboGuide directly uses 3D imaging, arising of visualization errors yielding wrong information about the vessel structure is more likely for our solution.

## References


[1] Emboguide - zur besseren behandlung von tumoren. `https://healthcare-in-europe.com/de/news/emboguide-zur-besseren-behandlung-von-tumoren.html`. Accessed: 2021-07-01.

[2] EmboGuide workflow-based embolization guidance. `https://www.usa.philips.com/healthcare/product/HCNCVC321/emboguide`. Accessed: 2021-07-01.

[3] Marengo Andrea, Rosso Chiara, and Bugianesi Elisabetta. Liver cancer: Connections with obesity, fatty liver, and cirrhosis. *Annual review of medicine*, 67:103–117, 1 2016.

[4] Bruce K Armstrong. Cancer epidemiology and prevention. *International Journal of Epidemiology*, 47:2097–2098, 12 2018.

[5] Yodit Abebe Ayalew, Kinde Anlay Fante, and Mohammed Aliy Mohammed. Modified u-net for liver cancer segmentation from computed tomography images with a new class balancing method. *BMC biomedical engineering*, 3(1), March 2021.

[6] bedros Taslakian, Ross Ingber, Eric Aaltonen, Jeremy Horn, and Ryan Hickey. 08 2019.

[7] Freddie Bray, Jacques Ferlay, Isabelle Soerjomataram, Rebecca L. Siegel, Lindsey A. Torre, and Ahmedin Jemal. Global cancer statistics 2018: Globocan estimates of incidence and mortality worldwide for 36 cancers in 185 countries. *CA: A Cancer Journal for Clinicians*, 68:394–424, 11 2018.

[8] Cammà Calogero, Schepis Filippo, Orlando Ambrogio, Albanese Maddalena, Shahied Lillian, Trevisani Franco, Andreone Pietro, Craxì Antonio, and Cottone Mario. Transarterial chemoembolization for unresectable hepatocellular carcinoma: meta-analysis of randomized controlled trials. *Radiology*, 224:47–54, 2002.

[9] Mei-Hwei Chen, Chien-Jen Lai, Mei-Shu Hsu, Hsu-Mei Wu, Tzee-Chung Kong, Man-Shan Liang, Der-Cherng Shau, Wen-Yi Chen, and Ding-Shinn Chang. Universal hepatitis b vaccination in taiwan and the incidence of hepatocellular carcinoma in children. taiwan childhood hepatoma study group. *The New England journal of medicine*, 336:1855–1859, 6 1997.

[10] Patrick Christ. Lits – liver tumor segmentation challenge (lits17). `https://competitions.codalab.org/competitions/17094`.

[11] Giorgio Lorenzo Colombo, Calogero Cammà, Adolfo Francesco Attili, Roberto Ganga, Giovanni Battista Gaeta, Giuseppina Brancaccio, Jean Marie Franzini, Marco Volpe, and Giuseppe Turchetti. Patterns of treatment and costs of intermediate and advanced hepatocellular carcinoma management in four italian centers. *Therapeutics and Clinical Risk Management*, 11:1603, 10 2015.

[12] Sigurdson ER, Ridge JA, Kemeny N, and Daly JM. Tumor and liver drug uptake following hepatic artery and portal vein infusion. *Journal of clinical oncology : official journal of the American Society of Clinical Oncology*, 5:1836–1840, 1987.

[13] Simon Esneault, Najah Hraiech, Eric Delabrousse, and Jean-Louis Dillenseger. Graph cut liver segmentation for interstitial ultrasound therapy. *Conference proceedings : ... Annual International Conference of the IEEE Engineering in Medicine and Biology Society. IEEE Engineering in Medicine and Biology Society. Conference*, 2007:5247–50, 02 2007.

[14] Simon Esneault, Najan Hraiech, Éric Delabrousse, and Jean Louis Dillenseger. Graph cut liver segmentation for interstitial ultrasound therapy. *Annual International Conference of the IEEE Engineering in Medicine and Biology - Proceedings*, pages 5247–5250, 2007.

[15] Deschamps F, Solomon SB, Thornton RH, Rao P, Hakime A, Kuoch V, and de Baere T. Computed analysis of three-dimensional cone-beam computed tomography angiography for determination of tumor-feeding vessels during chemoembolization of liver tumor: a pilot study. *Cardiovascular and interventional radiology*, 33:1235–1242, 12 2010.

[16] Jacques Ferlay, Hai-Rim Shin, Freddie Bray, David Forman, Colin Mathers, and Donald Maxwell Parkin. Estimates of worldwide burden of cancer in 2008: Globocan 2008. *International Journal of Cancer*, 127:2893–2917, 12 2010.

[17] Alejandro Forner, Josep M Llovet, and Jordi Bruix. Hepatocellular carcinoma. *The Lancet*, 379:1245–1255, 3 2012.

[18] N Howlader, AM Noone, M Krapcho, D Miller, K Bishop, CL Kosary, M Yu, J Ruhl, Z Tatalovich, A Mariotto, DR Lewis, HS Chen, EJ Feuer, and KA Cronin. Cancer statistics review, 1975-2014 - seer statistics, 2018.

[19] Jin Iwazawa, Shoichi Ohue, Naoko Hashimoto, and Takashi Mitani. Comparison of the number of image acquisitions and procedural time required for transarterial chemoembolization of hepatocellular carcinoma with and without tumor-feeder detection software. *Radiology Research and Practice*, 2013:1–6, 2013.

[20] Jin Iwazawa, Shoichi Ohue, Naoko Hashimoto, Osamu Muramoto, and Takashi Mitani. Clinical utility and limitations of tumor-feeder detection software for liver cancer embolization. *European Journal of Radiology*, 82:1665–1671, 10 2013.

[21] Titinunt Kitrungrotsakul, Xian-Hua Han, Yutaro Iwamoto, Lanfen Lin, Amir Hossein Foruzan, Wei Xiong, and Yen-Wei Chen. Vesselnet: A deep convolutional neural network with multi pathways for robust hepatic vessel segmentation. *Computerized Medical Imaging and Graphics*, 75:74–83, 2019.

[22] Josep M. Llovet, Maria Isabel Real, Xavier Montaña, Ramon Planas, Susana Coll, John Aponte, Carmen Ayuso, Margarita Sala, Jordi Muchart, Ricard Solà, Joan Rodés, and Jordi Bruix. Arterial embolisation or chemoembolisation versus symptomatic treatment in patients with unresectable hepatocellular carcinoma: A randomised controlled trial. *Lancet*, 359:1734–1739, 5 2002.

[23] Soler Luc, Hostettler Alexandre, Agnus Vincent, Charnoz Arnaud, Fasquel Jean-Baptiste, Moreau Johan, Osswald Anne-Blandine, Bouhadjar Mourad, and Marescaux Jacques. 3d image reconstruction for comparison of algorithm database: A patient specific anatomical and medical image database. `http://www.ircad.fr/softwares/3Dircadb/3Dircadb.php?lng=en`.

[24] Llovet Josep M., Brú Concepció, and Bruix Jordi. Prognosis of hepatocellular carcinoma: the bclc staging classification. *Seminars in liver disease*, 19:329–337, 1999.

[25] Fausto Milletari, Nassir Navab, and Seyed-Ahmad Ahmadi. V-net: Fully convolutional neural networks for volumetric medical image segmentation. pages 565–571. Institute of Electrical and Electronics Engineers Inc., 6 2016.

[26] Fausto Milletari, Nassir Navab, and Seyed-Ahmad Ahmadi. V-net: Fully convolutional neural networks for volumetric medical image segmentation. pages 565–571, 10 2016.

[27] Martyn Plummer, Catherine de Martel, Jerome Vignat, Jacques Ferlay, Freddie Bray, and Silvia Franceschi. Global burden of cancers attributable to infections in 2012: a synthetic analysis. *The Lancet Global Health*, 4:e609–e616, 9 2016.

[28] Loffroy R, Lin M, Rao P, Bhagat N, Noordhoek N, Radaelli A, Blijd J, and Geschwind JF. Comparing the detectability of hepatocellular carcinoma by c-arm dual-phase cone-beam computed tomography during hepatic arteriography with conventional contrast-enhanced magnetic resonance imaging. *Cardiovascular and interventional radiology*, 35:97–104, 2 2012.

[29] Ashwin Rammohan, Jeswanth Sathyanesan, Sukumar Ramaswami, Anand Lakshmanan, Perumal Senthil-Kumar, Ulagendra Perumal Srinivasan, Ravi Ramasamy, and Palaniappan Ravichandran. Embolization of liver tumors: Past, present and future. *World Journal of Radiology*, 4:405, 2012.

[30] Felix Ritter, Christian Hansen, Volker Dicken, Olaf Konrad, Bernhard Preim, and Heinz Otto Peitgen. Real-time illustration of vascular structures. *IEEE Transactions on Visualization and Computer Graphics*, 12:877–884, 9 2006.

[31] Ochs Robert. 510(k) premarket notification submission. `https://www.accessdata.fda.gov/cdrh_docs/pdf14/K142273.pdf`, 2015.

[32] Ochs Robert. 510(k) premarket notification submission. `https://www.accessdata.fda.gov/cdrh_docs/pdf16/K163285.pdf`, 2017.

[33] Olaf Ronneberger, Philipp Fischer, and Thomas Brox. U-net: Convolutional networks for biomedical image segmentation. volume 9351, pages 234–241, 5 2015.

[34] Nassir Rostambeigi, Adrienne S. Dekarske, Erin E. Austin, Jafar Golzarian, and Erik N. Cressman. Cost effectiveness of radioembolization compared with conventional transarterial chemoembolization for treatment of hepatocellular carcinoma. *Journal of Vascular and Interventional Radiology*, 25:1075–1084, 7 2014.

[35] Miyayama S, Yamashiro M, Hashimoto M, Hashimoto N, Ikuno M, Okumura K, Yoshida M, and Matsui O. Identification of small hepatocellular carcinoma and tumor-feeding branches with cone-beam ct guidance technology during transcatheter arterial chemoembolization. *Journal of vascular and interventional radiology : JVIR*, 24:501–508, 4 2013.

[36] D. Selle, B. Preim, A. Schenk, and H.-O. Peitgen. Analysis of vasculature for liver surgical planning. *IEEE Transactions on Medical Imaging*, 21(11):1344–1357, 2002.

[37] Luc Soler, Stéphane Nicolau, Patrick Pessaux, Didier Mutter, and Jacques Marescaux. Real-time 3d image reconstruction guidance in liver resection surgery. *Hepatobiliary surgery and nutrition*, 3:73–81, 04 2014.

[38] Keith Stuart. Chemoembolization in the management of liver tumors. *The Oncologist*, 8:425–437, 10 2003.

[39] Mills Thalia. syngo embolization guidance. `https://www.siemens-healthineers.com/angio/options-and-upgrades/clinical-software-applications/syngo-embolization-guidance`.

[40] Minami Y, Yagyu Y, Murakami T, and Kudo M. Tracking navigation imaging of transcatheter arterial chemoembolization for hepatocellular carcinoma using three-dimensional cone-beam ct angiography. *Liver cancer*, 3:53–61, 4 2014.

[41] Jinzhu Yang, Meihan Fu, and Ying Hu. Liver vessel segmentation based on inter-scale v-net. *Mathematical Biosciences and Engineering*, 18:4327–4340, 05 2021.

[42] Park YN, Yang CP, Fernandez GJ, Cubukcu O, Thung SN, and Theise ND. Neoangiogenesis and sinusoidal "capillarization" in dysplastic nodules of the liver. *The American journal of surgical pathology*, 22:656–662, 1998.

[43] Yi Zhang, Xiwen Pan, Congsheng Li, and Tongning Wu. 3d liver and tumor segmentation with cnns based on region and distance metrics. *Applied Sciences*, 10(11), 2020.